

# A Procedure for Post-Earthquake Damage Estimation Based on Detection of High-Frequency Transients

Aleksandar Zhelyazkov, Daniele Zonta Helmut Wenzel, Peter Furtner

**Abstract**—In the current research structural health monitoring is considered for addressing the critical issue of post-earthquake damage detection. A non-standard approach for damage detection via acoustic emission is presented -acoustic emissions are monitored in the low frequency range (up to 120 Hz). Such emissions are termed high-frequency transients. Further a damage indicator defined as the Time-Ratio Damage Indicator is introduced. The indicator relies on time-instance measurements of damage initiation and deformation peaks. Based on the time-instance measurements a procedure for estimation of the maximum drift ratio is proposed. Monitoring data is used from a shaking-table test of a full-scale reinforced concrete bridge pier. Damage of the experimental column is successfully detected and the proposed damage indicator is calculated.

**Keywords**—Acoustic emission, Damage detection, Shaking table test, Structural health monitoring, High-frequency transients.

## I. INTRODUCTION

**E**FFICIENT and reliable procedures for post-earthquake damage assessment (PEDA) of civil structures have long been a topic of interest for property owners, state officials and as a result for many researchers. One approach for addressing the issue of PEDA is the implementation of a structural health monitoring system (SHM) [1]. Consequently, output measurements from time-segments before, during and after the earthquake event could be processed with the purpose of identifying signs in the response indicative of damage. The procedure which is used for processing the measurement output is in essence the damage detection method. A method would be considered reliable if it allows the timely identification of structural performance (Immediate Occupancy, Life Safety, Collapse prevention - Figure 1, [2]).

Generally damage detection methods branch out in two main directions - identification of permanent response

A. Zhelyazkov is with the Department of Civil, Environmental and Mechanical Engineering, University of Trento, Trento and a Structural Engineer at Vienna Consulting Engineers, 38123 Italy (e-mail: zhelyazkov@vce.at).

D. Zonta is with the Department of Civil and Environmental Engineering, University of Strathclyde, Glasgow, G1 1XQ United Kingdom (e-mail: danielle.zonta@strath.ac.uk).

H. Wenzel is the Managing Director of Wenzel Consulting Engineers, Vienna, A 1180 Austria (e-mail: helmut.wenzel@wenzel-consult.com).

P. Furtner is an Authorized Representative of Vienna Consulting Engineers, Vienna, A1030 Austria (e-mail: furtner@vce.at).

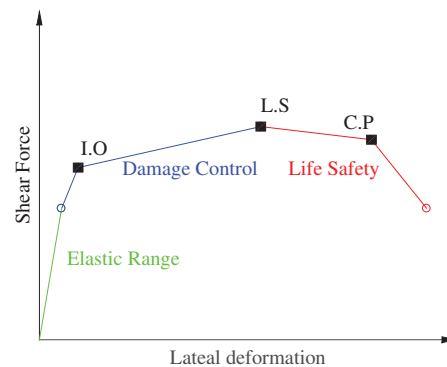


Fig. 1 Performance levels according to FEMA274 [2]

characteristics and identification of transient response characteristics.

Methods based on identification of permanent changes in the character of the response (vibrational methods) are most commonly used. The character of the response is dependent on the modal properties of the structures and changes of these properties is most often indicative of stiffness reduction and hence occurrence of damage [3]. A frequent issue with these methods is the low sensitivity of the modal parameters to the occurrence of damage. In addition the identified modal properties are influenced from factors, such as external loading to the structure and temperature changes. Nevertheless, these factors could be compensated for by additional statistical processing of the data [4].

Damage detection methods relying on identification of transient response are herein subdivided - identification of the temporary threshold exceedance of a certain Engineering Demand Parameter (EDP), such as drift ratio, and identification of high-frequency transients related to damage.

Drift ratio measurement is a well-established procedure and is done by double-integration of acceleration record at the top and bottom of the structural element. Issues could arise from potential loss of the plastic part of the response due to base-correction [5] and the relatively high instrumentation density required to capture the response of the structure [6].

Methods based on detection of high-frequency transients are further subdivided according to the expected frequency range of the monitored transients.

The general acoustic emission (AE) approach requires a sampling rate in the order of hundreds of kilohertz. This allows the detection of elastic waves generated due to a sudden release of internal energy within the volume of the monitored structure [7]. Such elastic waves could be generated, for example, from initiation of concrete cracking. Damage is often characterized by the "hit" number [8]. These methods are much more sensitive to damage than vibrational methods, but when it comes to civil structures, an apparent issue is the fast distance attenuation of the acoustic waves. Therefore, parts of the acoustic signal could be lost depending on the distance between the location of damage and the instrument [9]. This makes the method location dependent since e.g. the "hit" number changes and implies the necessity for a dense instrumentation mesh in order for the global damage state of the structures to be induced.

Transients in the lower frequency ranges attenuate slower with distance and therefore are more applicable to civil engineering purposes. These transients are expected to affect the response of the structures in the modes governing its global response. They are termed as High-Frequency Transients (HFT), but it should be pointed out that transients monitored in AE are in higher frequency ranges (daHz vs. kHz). A procedure for fracture detection in welded steel moment frames based on identification of damage related HFT's is presented in [10]. Investigations of HFT for a steel frame- reinforced concrete shear wall building are carried out in [11].

The current research presents a procedure for assessment of damage level based on measurement of HFT arrival times and their distance forward in time to the closest deformation extremum. It is assumed that the structure accumulates damage in the time-window between the arrival of the HFT and the deformation extremum. Additionally, a damage indicator is proposed, which is the ratio between the maximum value of a chosen EDP and the value of the EDP at the arrival time of the first HFT. The damage indicator is defined as the Time-Ratio Damage Indicator (TRDI).

## II. DEDUCTION OF THE TIME-RATIO DAMAGE INDICATOR

The TRDI is deduced with the help of several main assumptions: i) The structure accumulates damage in the time-window between the arrival of the HFT and the closest upcoming deformation extremum ii) The structure has a predominant first mode response iii) The estimation of the maximum EDP could be done independently for opposite directions of structural response.

Global response is herein understood to be the part of the response containing only modes defining the global response of the structure and not the transient part.

Based on the above assumptions a hypothetical response is presented on Figure 2. The upper part of the figure presents the assumed global response per direction and the lower part presents the expected HFT's. As already discussed, the structure starts to accumulate damage at the arrival time

of the HFT and accumulates damage until the deformation extremum is reached.  $\Theta'$  is the value of the EDP at which the first HFT arrived,  $\Theta_{max,i}$  is the maximum estimated value of the EDP during a deformation half-cycle with a HFT present,  $\tau_i$  is the time-window of damage accumulation in the  $i$ -th half-cycle and  $T'_i$  is the time-length of the deformation cycle. It is also assumed that iv) the structure continues to accumulate damage once  $\Theta_{max,i}$  is exceeded.

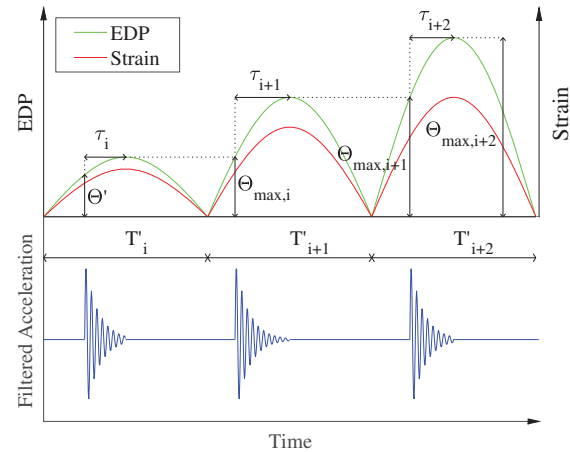


Fig. 2 Visualizing the TRDI

If the value of  $\Theta'$  is known then we could obtain  $\Theta_{max,i}$  with the following relation:

$$\Theta_{max,i} = \frac{\Theta'}{\sin\pi(\frac{1}{2} - \frac{\tau_i}{T'_i})} \quad (1)$$

The maximum value of the EDP in the following cycle with a HFT present is:

$$\Theta_{max,i+1} = \Theta_{max,i} \{csc\pi(\frac{1}{2} - \frac{\tau_{i+1}}{T'_{i+1}})\} \quad (2)$$

The maximum value of the EDP after the last HFT is:

$$\Theta_{max,N} = \Theta' \prod_{i=1}^N \{csc\pi(\frac{1}{2} - \frac{\tau_{i+1}}{T'_{i+1}})\} \quad (3)$$

where  $N$  is the number of HFT's. The damage indicator  $TRDI$  is defined as:

$$TRDI = \prod_{i=1}^N \{csc\pi(\frac{1}{2} - \frac{\tau_{i+1}}{T'_{i+1}})\} \quad (4)$$

and gives the ratio between the maximum EDP of the structure and the EDP at which the structure first starts to damage. As apparent from equation 3, the value of  $\Theta'$  would have to be known in order to obtain  $\Theta_{max,N}$ .

The naming of the damage indicator (Time Ratio Damage Indicator) follows from the variable in equation 4, which is a ratio between duration of damage ( $\tau$ ) and duration of the half-cycle ( $T'_i$ ).

### III. CASE-STUDY CALCULATION OF THE TRDI

In this section a case-study calculation of the TRDI is demonstrated on an output data from an experimental reinforced concrete column (Fig. 3) tested on a shaking table [12]. Additionally a step-by-step procedure is provided for the calculation of the TRDI.

#### A. Description of the Shaking Table Experiment

A circular reinforced concrete column was tested on a shaking table. The height of the column was 7,31 meter and the diameter was 1,22 meter. A top weight of 2,32 MN was included by post-tensioned together reinforced concrete blocks. The column was designed according to the Caltrans seismic design guidelines [13]. 10 significant ground motions (EQ's) were induced at the base of the column (Table I). Displacement relative to the base was measured by horizontal spring potentiometers attached to the column and a stiff steel structure which was also mounted on the table. Drift is obtained by dividing the measured relative displacement by the height of the column. Accelerometers and strain-gauges were also installed along the height of the column. The sampling rate of the monitoring system was 240 Hz.



Fig. 3 Test set-up [12]

#### B. Calculating the TRDI

The TRDI of the experimental column is obtained according to the following steps:

- 1) Filter a measured acceleration from an accelerometer placed along the height of a structure with a high-pass filter. The cut-off frequency of the filter should be high enough to remove the contribution of the global modes (50 Hz in this case).
- 2) Apply Short-Time Fourier Transform (STFT) on the filtered acceleration (Figure 5).
- 3) Pin-point the damage instances (HFT's) for the filtered acceleration in the time-frequency and time-domain representations (Figure 5 and Figure 6).

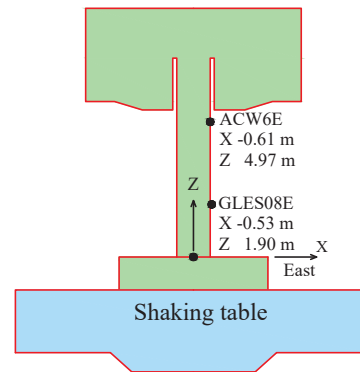


Fig. 4 Position of the instruments used for calculating the TRDI

- 4) Filter the strain gauge data with a low-pass filter. The cut-off frequency should be low enough, so that only the contribution of the global modes remains. (25 Hz in this case).
- 5) Plot together the filtered acceleration and strain gauge data (Figure 6)
- 6) Measure damage duration  $\tau_i$  and  $T'_i$  from Figure 6 in order calculate the  $TRDI$  from Equation 4.

Measurement output was used from accelerometer ACW6E for capturing HFT's and strain gauge data from GLES08E was used for measuring time instances of deformation extrema (Figure 4).

The purpose of the strain gauge is to capture the time instances of EDP extrema. For this case-study drift ratio was the considered EDP. It is expected that the extrema of the drift ratio and strain coincide in time, therefore the strain gauge is suitable for capturing time instances of drift ratio extrema.

It was observed that only the accelerometers are able to capture the HFT's, even though the strain gauge data was sampled at the same rate. The reason for this could be a transient rigid rotation of the column about the location of damage at the time instances of damage initiation. Rigid body response could be captured only with an accelerometer and not a strain gauge. On the other hand, a single accelerometer can not capture relative deformation extrema and therefore a strain gauge is required.

#### C. Results

The goal is to estimate the maximum drift ratio in each half-cycle of observed HFT and compare the estimation with the drift measured with spring potentiometers. Therefore it is required to calculate the TRDI for each half-cycle with observed damage an multiply it with the drift ratio at the time of the first observed HFT ( $\Theta'$ ). In a real-case scenario  $\Theta'$  would not be available (further discussed in Section ??), but in this case this value was taken from the potentiometer measurements and used as input to estimate the rest of the drifts.

TABLE I  
 DESCRIPTION OF SHAKE TABLE TEST AND OBSERVED DAMAGE

Ground motion	Description	Notes on outcome
EQ1	Agnew State Hospital record 1989 Loma Prieta	Residual cracks footing-to-column interface 0.1 mm
EQ2	Coralitos 1989 Loma Prieta earthquake	Residual cracks in the column are marked
EQ3	Los Gatos Center 1989 Loma Prieta earthquake	Spalling on the West face of the column
EQ4	Coralitos 1989 Loma Prieta earthquake	More spalling on the West face
EQ5	Takatori at -80% amplitude 1995 Kobe earthquake	Continued spalling. Longitudinal bars are visible
EQ6	Los Gatos Center 1989 Loma Prieta earthquake	-not available
EQ7	Takatori at 100% amplitude 1995 Kobe earthquake	-not available
EQ8	Takatori at -120% amplitude 1995 Kobe earthquake	Two longitudinal rebar fracture East face
EQ9	Takatori at 120% amplitude 1995 Kobe earthquake	Longitudinal rebar fracture on East and West face
EQ10	Takatori at 120% amplitude 1995 Kobe earthquake	Impacted the East safety restraint

TABLE II  
 CALCULATION OF TRDI FOR EACH EQ

EQ #	EQ1	EQ2	EQ2	EQ3	EQ3
HFT #	1	2	3	4	5
$t_1$ [s]	22.762	23.937	24.429	28.879	31.487
$t_2$ [s]	23.271	24.429	24.910	29.400	32.396
$t_d$ [s]	23.125	24.333	24.73	29.220	32.010
$\tau_i$ [s]	0.146	0.096	0.180	0.180	0.386
$T'_i$ [s]	0.509	0.492	0.481	0.521	0.909
$TRDI_i$	1.611	1.967	-2.597	-5.567	8.380
$\Theta'(t_d)$ [%]	0.520	0.690	-0.530	-1.000	0.760
$\Theta'_{max,i}$ [%]	0.710	0.790	-1.040	-1.760	5.050
$\Theta_{max,i}$ [%]	0.838	1.024	-1.377	-2.951	4.367

First the arrival times of the HFT's are located in time from the time-frequency representation and time-domain representation (Fig.5, Fig.6). Deformation extrema are identified from the filtered strain gauge data.  $\tau_i$  and  $T'_i$  are obtained according to the following formulas:

$$\tau_i = t_2 - t_d \quad (5)$$

$$T' = t_2 - t_1 \quad (6)$$

, where  $t_d$  is the arrival time of the HFT in the 1-th cycle of response.  $t_1$  and  $t_2$  are the time instances of response extrema correspondingly before and after the HFT in a given half-cycle (Figure 6).

Finally the results are summarized on Figure 7 and Table II.  $\Theta'_{max,i}$  is the maximum drift ratio per cycle measured with spring potentiometers and serves as comparison with the estimated maximum drift ratio ( $\Theta_{max,i}$ ).

There are 5 HFT's observed. The plus and minus signs in II indicate the direction of deformation of the column. For each direction of deformation the EDP (drift ratio) is estimated separately, which is in accordance with assumption iii) (Section II).

#### IV. DISCUSSION OF RESULTS

The experimental data indicates that the directly measured (using spring potentiometers) and theoretically estimated values of the drift ratio are in good agreement. A good match is expected due to the predominant first mode response of the structure. A predominant first mode leads to a response, which within a half-cycle could be approached by a harmonic function. This allows the estimation of maximum drifts with equation 3. The accuracy of the estimated values

is expected to deteriorate if the contribution of the higher modes is more significant.

It was further observed that initiation of damage could be detected in the early stages. The first HFT was captured at a drift ratio of approximately 0.5%, which is expected to be below the Immediate Occupancy Performance level [2]. No changes in the modal parameters of the structure were observed at the early stages of damage initiation, indicating that traditional vibrational methods are less sensitive to damage than the currently proposed approach.

The HFT's were detected from every accelerometer on the column, demonstrating that distance attenuation is not an issue, at least for the structure of the considered size. Further, a sensitivity analysis was conducted calculating the TRDI for different pairs of accelerometers and strain-gauges. Results show little dependence on instrument location, which is an important prerequisite for the estimation of the global damage state of the structure. The TRDI is also rather insensitive to the chosen cut-off frequencies of the filters, as long as guidelines laid out in Section III-B are followed.

A sample overlap of 1 was considered for the current calculation of the STFT. As expected, an increase in the sample overlap would lead to a decrease in accuracy of measured arrival times of the HFT's.

It is evident that there is a correlation between occurrence of high frequencies and column damage. Nevertheless, one should take special care as "correlation does not imply causation". This is apparent from the column response at EQ4 - part of the high frequencies observed are due to the frequency content of the induced base motion, but no damage should have occurred since, according to the spring potentiometer measurements, the drift from EQ3 was not exceeded. Transients are observed since due to previous damage the energy of the response is now shifted to higher modes. This means that after a certain damage level the transients contained in the base excitation are transferred to the upper part of the column with larger amplitudes. As a result it becomes cumbersome to differentiate between transients caused by damage initiation and transients contained in the base excitation, which was the reason for calculating the TRDI only up to EQ3.

Shift of vibrational energy from lower to higher with the accumulation of damage is researched in [14] and [15].



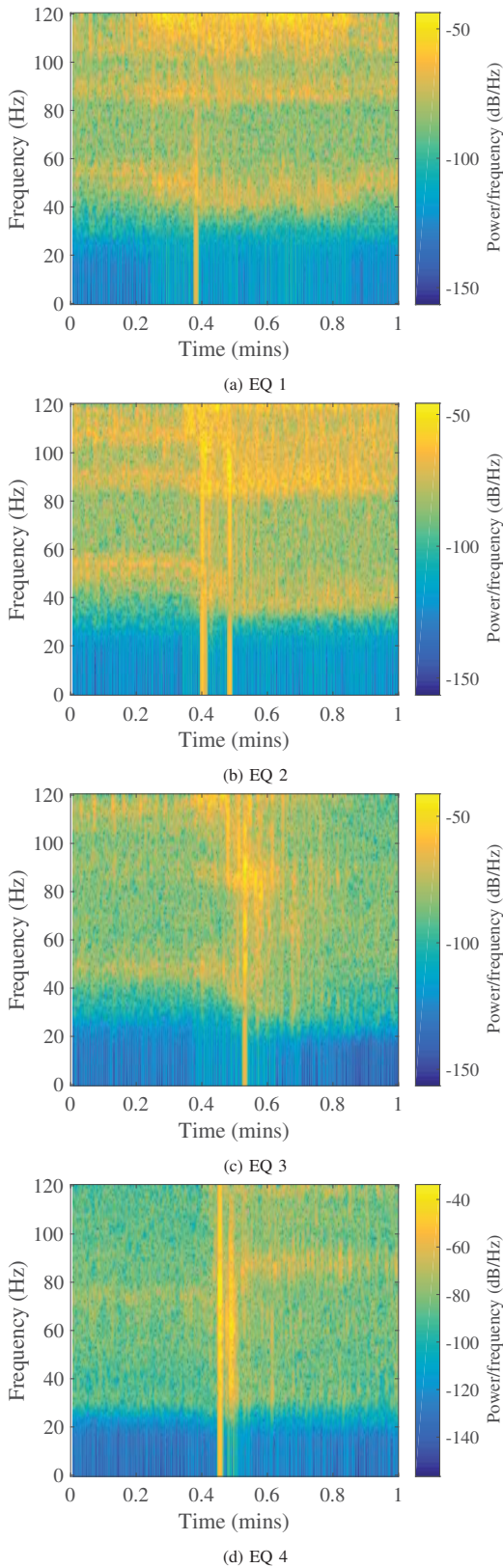


Fig. 5 Spectrograms of the filtered accelerations

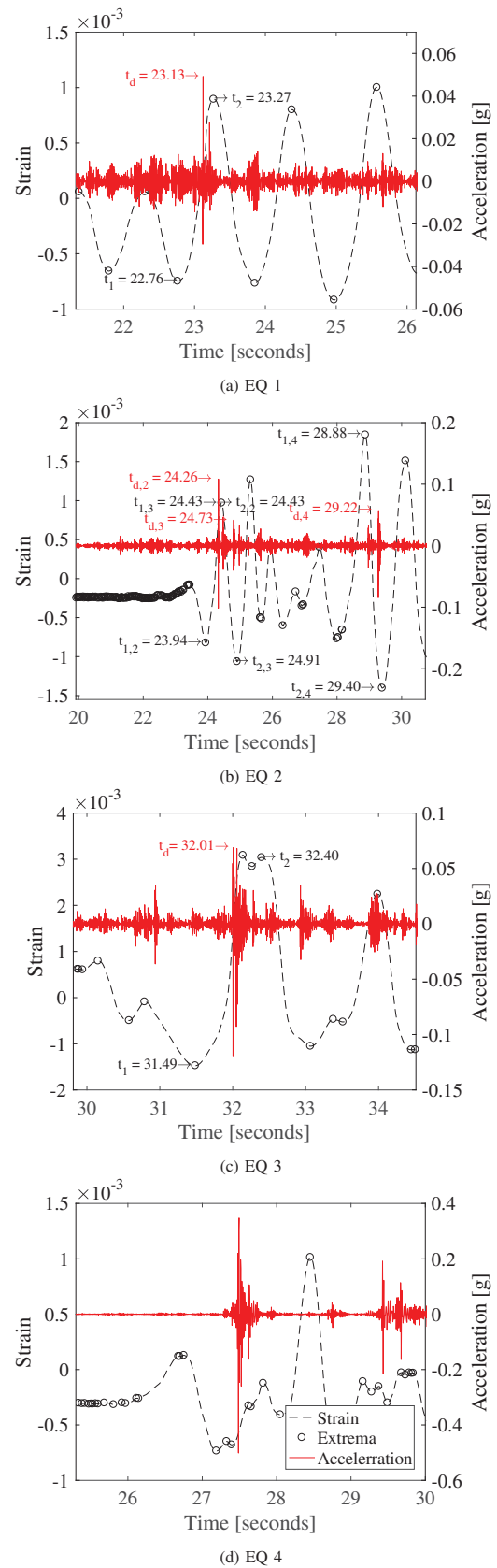


Fig. 6 Filtered accelerations and strains in the time domain

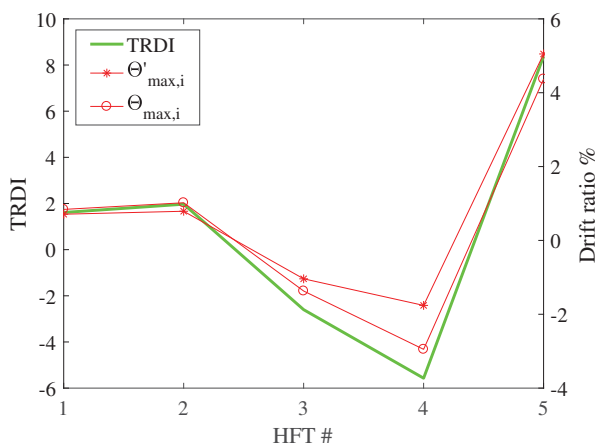


Fig. 7 TRDI versus Drift Ratio

### V. LIMITATIONS OF THE PROPOSED PROCEDURE

A notable limitation is the requirement to have an estimation of  $\Theta'$  (the drift at which the first HFT was observed) in order to estimate the maximum drift. If  $\Theta'$  is not available then only the *TRDI* could be calculated, but based solely on the *TRDI* the performance level could not be currently estimated.

A further limitation is a requirement for a predominant first mode response of the structure. In case this requirement is not met the drift deduced from the *TRDI* will be inaccurate. This follows from the presumption of sinusoidal response as a basis for the deduction of the *TRDI* (Section 2).

### VI. SUMMARY AND CONCLUSIONS

A damage indicator to be obtained for output instrumentation data was introduced (Time-Ratio Damage Indicator). The indicator relies entirely on the measured arrival times of damage related HFT's and time instances of deformation peaks. A case study calculation was performed with data from an experimental reinforced concrete column. Damage initiation was captured by observing the response of the structure in the higher frequency bands (50 – 120 Hz). The maximum deformation peaks were measured from strain-gauge data. The time difference between damage initiation and peak deformation is assumed to be the duration of damage. In a final step the *TRDI* is calculated and results show that the *TRDI* grows proportionally with the measured drift ratio.

Another observation was the low sensitivity of the *TRDI* to the location of the instruments for the tested column. This follows from the fact that the measured arrival times of the HFT's (related to damage) and the measured instances of deformation peaks differ insignificantly with instrument location. It should be noted again that this is an observation only for the experimental column analyzed above. As discussed, the global damage state of the structure is of interest and low sensitivity to location of the measurement instruments is a prerequisite.

There are potential advantages when comparing the *TRDI* with accelerometer measured interstory drift (double integration of the measured acceleration). Reduction in instrumentation density could be achieved, since HFT could be detected and *TRDI* calculated even if the accelerometer and strain gauge are not directly attached to the affected structural element. Further research is required in order to assess the location dependence of the proposed procedure for larger structures. It was additionally elaborated upon the advantage of HFT compared to typical AE approaches with regard to distance attenuation. Lower frequency waves attenuate slower with distance. Since it is of general interest to monitor the global damage state of an entire civil structure, fast attenuation with distance is an issue. Such attenuation is observed for waves in the frequency ranges typically used in AE monitoring, which implies the necessity for a dense instrumentation mesh.

No changes were observed in the modal properties of the column for low levels of damage (Immediate Occupancy). This confirms the expectation that traditional vibrational methods are less sensitive to damage than methods relying on detection of transient response.

It was further observed that the HFT's are not occurring exactly at the moment of concrete cracking, but at a later stage. This is expected, since with the given sampling rate (240 Hz) the elastic waves generated directly from the concrete cracking, which are in the frequency range of 40-70 kHz, could not be captured. Additionally, the captured HFT response is expected to contain rigid body modes, since the transients are detected by the accelerometers and not the strain gauges. The above observations lead to the hypothesis that the captured HFT's could be caused by loss of bond between the reinforcement and concrete. Such a damage mechanism is expected to cause partial rigid body response.

Future research should be aimed at understanding the exact damage mechanism causing the HFT's. It would be also beneficial to implement the above procedure on measurement data with a higher sampling rate.

### ACKNOWLEDGMENT

This work has received funding from the European Union's Horizon 2020 research and innovation program under the Marie Skłodowska-Curie grant agreement No 721816. The research was performed as part of project XP-Resilience coordinated by the University of Trento, Italy.

### REFERENCES

- [1] M. Celebi, Seismic monitoring of structures and new developments, in: Earthquakes and health monitoring of civil structures, Springer, 2013, pp. 37–84.
- [2] NEHRP Commentary on the Guidelines For Seismic Rehabilitation of Buildings, Standard, Federal Emergency Management Agency, Washington, D.C (Oct. 1997).
- [3] D. Zonta, A. Elgamal, M. Fraser, M. N. Priestley, Analysis of change in dynamic properties of a frame-resistant test building, *Engineering Structures* 30 (1) (2008) 183–196.
- [4] A. Kita, N. Cavalagli, F. Ubertini, Temperature effects on static and dynamic behavior of consoli palace in gubbio, italy, *Mechanical Systems and Signal Processing* 120 (2019) 180–202.

- [5] M. I. Todorovska, M. D. Trifunac, Earthquake damage detection in the imperial county services building i: The data and time–frequency analysis, *Soil Dynamics and Earthquake Engineering* 27 (6) (2007) 564 – 576.
- [6] An alternative procedure for seismic analysis and design of tall buildings located in the Los Angeles region, Document, Los Angeles Tall Buildings Structural Design Council, Los Angeles, C.A (Mar. 2018).
- [7] A. G. Beattie, Acoustic emission non-destructive testing of structures using source location techniques, Albuquerque and Livermore.
- [8] F. Sagasta, M. E. Zitto, R. Piotrkowski, A. Benavent-Climent, E. Suarez, A. Gallego, Acoustic emission energy b-value for local damage evaluation in reinforced concrete structures subjected to seismic loadings, *Mechanical Systems and Signal Processing* 102 (2018) 262–277.
- [9] F. Sagasta, Y. Mizutani, I. Valverde, E. Suarez, J. R. Francisco, A. Gallego, Influence of attenuation on the acoustic emission b-value for damage evaluation of reinforced concrete specimens.
- [10] J. E. Rodgers, M. Çelebi, Method for detecting moment connection fracture using high-frequency transients in recorded accelerations, *Journal of Constructional Steel Research* 67 (3) (2011) 293–307.
- [11] P. Bodin, J. Vidale, T. Walsh, R. Çakir, M. Çelebi, Transient and long-term changes in seismic response of the natural resources building, Olympia, Washington, due to earthquake shaking, *Journal of Earthquake Engineering* 16 (5) (2012) 607–622.
- [12] M. Schoettler, J. Restrepo, G. Guerrini, D. Duck, F. Carrea, A full-scale, single-column bridge bent tested by shake-table excitation, Center for Civil Engineering Earthquake Research, Department of Civil Engineering, University of Nevada.
- [13] Seismic Design Criteria, Standard, California Department of Transportation, Sacramento, C.A (2006).
- [14] H. Wenzel, V. V. C. E. Z. G. Krims-Steiner, Industrial Safety and Life Cycle Engineering: Technologies, Standards, Applications ; IRIS, Chapter 3, VCE Vienna Consulting Engineers ZT GmbH, 2013.
- [15] A. Tributsch, C. Adam, An enhanced energy vibration-based approach for damage detection and localization, *Structural Control and Health Monitoring* 25 (1).